Time Evolution of the PSD in Crystallization Operations: An Analytical Solution based on Ornstein-Uhlenbeck Process

Giuseppe Cogoni, Massimiliano Grosso and Roberto Baratti
Dipartimento di Ingegneria Chimica e Materiali, Università degli Studi di Cagliari, Piazza D'Armi, I-09123, Cagliari, Italy

Jose A. Romagnoli
Dept. of Chemical Engineering, Louisiana State University, South Stadium Road, Baton Rouge, LA 70803

DOI 10.1002/aic.13760
Published online March 2, 2012 in Wiley Online Library (wileyonlinelibrary.com).

A new formulation of the recent stochastic approach for the description of the particle-size distribution (PSD) time evolution in antisolvent crystal-growth processes is presented. In this new approach, the crystals size is modeled as a random variable driven by a Gompertz growth term and the corresponding Fokker-Planck equation is carried out. This proposed formulation, allows an analytical solution to describe the time evolution of the PSD as a function of the model parameters. The analytical solution is obtained by exploiting the typical properties of linear partial differential equations with linear coefficients, and using the analogy with Kalman filter, in terms of the first two stochastic moments: mean and variance of the PSD. Furthermore, an alternative way for the parameters estimation based on the maximum likelihood estimation is also introduced. Validations against experimental data are provided for the NaCl-water-ethanol antisolvent crystallization system. © 2012 American Institute of Chemical Engineers *AIChE J,* 58: 3731–3739, 2012
Keywords: antisolvent crystallization, Fokker-Planck equation, Ornstein-Uhlenbeck process, maximum likelihood estimation

Introduction

Crystallization is a technique widely used for the production of pharmaceuticals, fertilizers and fine chemicals.[1–6] The development of effective mathematical models describing the crystal growth dynamics is a crucial issue toward finding the optimal process performance and to control the crystal size and distribution. This modeling is usually accomplished by resorting to population balances equations (PBE),[7] which may require a deep knowledge of the system, a consistent number of parameters and, in general, the solution of the model is obtained numerically.

Recently, direct design, model-free approaches were proposed as an alternative efficient way of controlling crystallization processes for antisolvent, cooling and combined processes and in general for particulate processes.[8–13] Along this way, Grosso et al.[14] proposed a simple model based on the Fokker-Plank equation (FPE) approach to model crystallization systems characterized by the particle-size distribution (PSD). In this approach, the time evolution of each element of the population, the crystal, was regarded as a possible outcome of a random variable driven by a nonlinear deterministic term. In particular, the logistic equation, appearing as a reasonable description of the average growth dynamics[14] was selected. The nonlinear term appearing in the logistic model leads to a resulting FPE that does not present an analytical solution, and, therefore, numerical integration was needed.

From a control, optimization and monitoring point of view the availability of the analytical solution of the model describing the time evolution of the PSD may be valuable for the design of proper offline and/or online model based control strategies. In this article we propose a new formulation for the deterministic model that allows obtaining the analytical solution of the resulting FPE. In particular, in the new formulation, the Gompertz[15] model is selected to describe the time evolution of the mean crystal size providing eventually a FPE with linear coefficients. By performing a suitable variable transformation, the problem can be reformulated as an Ornstein-Uhlenbeck process,[16] and the analytical solution is then obtained to describe the time evolution of the PSD as a function of the model parameters. The analytical solution is obtained by exploiting the typical properties of the linear partial differential equations with linear coefficients or using the analogy with the Kalman filter,[17] in terms of the first two stochastic moments: mean size of crystals and variance of the PSD. In fact, assuming a Gaussian initial PDF at time t_0, the transient PDF will remain Gaussian at any time $t = t_0$, and, therefore, it could be characterized by the first two moments.[16,17]

Furthermore, parameters estimation is performed by applying the maximum likelihood estimation method (ML) to obtain the parameters directly from the observed data.[18] This policy can lead to a straightforward inference of the parameters,

Correspondence concerning this article should be addressed to R. Baratti at baratti@dicm.unica.it.

without resorting to a preliminary estimation of the experimental PSD through, e.g., the development of a kernel based function.[14] In this way, the estimation error due by the introduction of the kernel basis function approximation is circumvented. In addition, the data sample needed to perform valuable parameter inference may be more parsimonious with respect to the previous approach.[19]

To evaluate the reliability of the proposed formulation, validations against experimental data for the NaCl-water-ethanol antisolvent crystallization system and the comparison with the previous model[14,19] is presented.

The Model

In the proposed formulation for the stochastic modeling, the crystals are classified by their size L, and the growth of each individual crystal is supposed to be independent by the other crystals, and is governed by the same deterministic model. In order to take into account the growth fluctuations and the unknown dynamics not captured by the deterministic term, a random component can be introduced as a geometric Brownian motion[14] GBM, where the intensity of the fluctuations depends linearly on the crystal size. It should be reminded that the GBM assumption is consistent with the law of proportionate effect (LPE),[19,20] which assesses that the rate of growth is proportional to the linear-size times a random number, thereby making growth rate size-dependent

$$\frac{dL}{dt} = h(L,t;\theta) + L\eta(t) \tag{1}$$

In Eq. 1, $h(L,t;\theta)$ is a function that describes the rate of growth, L is the size of the single crystal, t is the time, θ is the vector of parameters defined in the model, and $\eta(t)$ is a random term assumed as Gaussian additive white noise

$$\begin{cases} \langle \eta(t) \rangle = 0 \\ \langle \eta(t)\eta(t') \rangle = 2D\delta(t-t') \end{cases} \tag{2}$$

where D is the noise intensity. By performing a nonlinear suitable variable transformation $y = \ln(L)$, the fluctuation term does not depend anymore on the crystal size[14]

$$\frac{1}{L}\frac{dL}{dt} = \frac{d\ln L}{dt} = \frac{1}{L}h(L,t;\theta) + \eta(t) \overset{(y=\ln L)}{=} \frac{dy}{dt} = h'(y,t;\theta) + \eta(t) \tag{3}$$

The evolution in time of the probability density function $\Psi(y,t)$ related to the random variable y is described by the FPE[16]

$$\frac{\partial \Psi(y,t)}{\partial t} = D\frac{\partial^2 \Psi(y,t)}{\partial y^2} - \frac{\partial}{\partial y}[\Psi(y,t)h(y,t;\theta)] \tag{4}$$

along with the boundary conditions

$$\frac{\partial \Psi(-\infty,t)}{\partial y} = 0 \tag{5}$$

$$\frac{\partial \Psi(+\infty,t)}{\partial y} = 0 \tag{6}$$

and the initial conditions, hereafter assumed as a Gaussian distribution

$$\Psi(y,t_0) = \frac{1}{\sigma_0\sqrt{2\pi}} exp\left[-\frac{(y-\mu_0)^2}{2\sigma_0^2}\right] \tag{7}$$

where μ_0 and σ_0 are, respectively, the mean and variance of the distribution at time $t = t_0$. The FPE (Eq. 4) contains two conceptually different terms: the drift term, $\partial[g(y,t)\Psi]/\partial y$, takes into account the deterministic contribution on the growth process (roughly speaking, the dynamics of the population average). Conversely, the diffusive term $D\ \partial^2\psi/\partial y^2$, determines the random motion of the variable y related to fluctuations in the particle growth process.[14]

Drift term based on the logistic equation (LG)

In the following, the stochastic model based on the logistic equation introduced in Grosso et al.[14,19] is briefly summarized, hereafter referred as the LG model. In such formulation the deterministic growth model is assumed to follow a Logistic equation. Thus, the growth term is

$$h'(y,t;\theta) = ry\left(1 - \frac{y}{K}\right) \tag{8}$$

where r is the crystal growth rate constant, and K is the equilibrium logarithmic mean crystal size.[14,16] The corresponding FPE becomes

$$\frac{\partial \Psi(y,t)}{\partial t} = D\frac{\partial^2 \Psi(y,t)}{\partial y^2} - \frac{\partial}{\partial y}\left[\Psi(y,t)\left(ry\left(1-\frac{y}{K}\right)\right)\right] \tag{9}$$

The nonlinear drift term has some implications on the solution characteristics. In fact, it allows capturing the occurrence of distortions from the ideal symmetric case in the PSD solution $\Psi(y,t)$ for any time. The main drawback is that an analytical solution for the transient FPE is not available and a numerical integration is eventually required.[14]

Drift term based on the Gompertz equation (GZ)

In this novel approach, the deterministic term, $h(L;\theta)$, is here assumed as a Gompertz model (GZ)[15]

$$h(L;\theta) = -rLln\frac{L}{L_0} \tag{10}$$

In the absence of noise ($\eta(t) = 0$) the model in Eq. 1 shows some qualitative analogies with the logistic model: the system tends toward a unique stable stationary solution corresponding at $L = L_0$, which correspond to the asymptotic mean crystal size observed in the experimental runs and the crystals growth rate constant is given by r. Following the same approach used with the LG model, see Eq. 3, Eq. 10 can be further manipulated

$$\frac{1}{L}\frac{dL}{dt} = \frac{dlnL}{dt} = -r(lnL - lnL_0) + \eta(t) \tag{11}$$

and applying the variable transformation $y = \ln(L)$, a stochastic equation can be devised for the random variable y

$$\frac{dy}{dt} = h'(y;\theta) + \eta(t) = v\left(1 - \frac{y}{K}\right) + \eta(t) \tag{12}$$

where $K = \ln(L_0)$ and $v = r\ln(L_0)$. Equation 12 corresponds to a Ornstein-Uhlenbeck process (OUP),[16] where the stochastic term $\eta(t)$ follows Eq. 2, with a constant diffusion coefficient D,

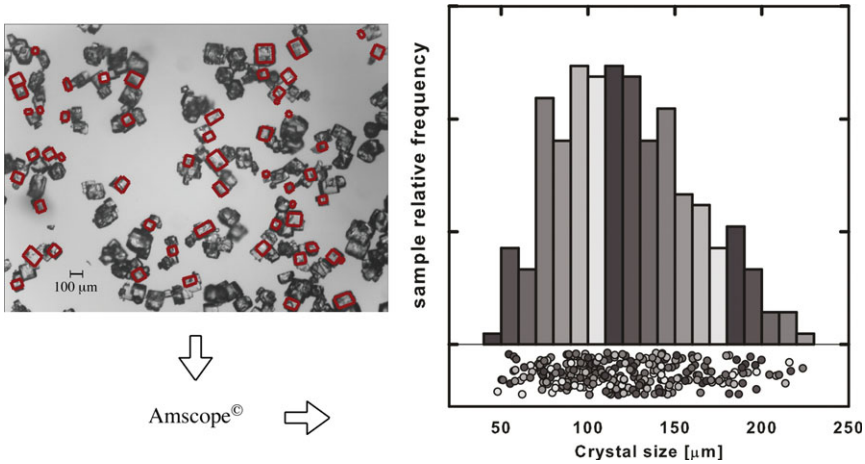

Figure 1. Flow sheet of the data size acquisition through visual inspection.

[Color figure can be viewed in the online issue, which is available at wileyonlinelibrary.com.]

and the drift term depends linearly on the state variable y. The corresponding FPE is then

$$\frac{\partial \Psi(y,t)}{\partial t} = D\frac{\partial^2 \Psi(y,t)}{\partial y^2} - v\frac{\partial}{\partial y}\left[\left(1-\frac{y}{K}\right)\Psi(y,t)\right] \tag{13}$$

The domain definition of Eq. 13 is the same of Eq. 9, i.e., $t \in (t_0, +\infty)$ and $y \in (-\infty, +\infty)$. The initial condition for $t = t_0$ may be assumed as a normal distribution

$$\Psi(y,t_0) = \frac{1}{\sigma_0\sqrt{2\pi}} exp\left[-\frac{(y-\mu_0)^2}{2\sigma_0^2}\right] \tag{14}$$

Analytical solution of the gompertz model (GZ)

It can be demonstrated that, when dealing with a Ornstein-Uhlenbeck process (Eq. 12), and the initial conditions are assumed to be Gaussian (see Eq. 14), the form of the PDF will stay Gaussian at any time.[16,17] Thus, the first two moments of the distribution: mean, $\mu(t)$, and variance, $\sigma^2(t)$ uniquely identify the probability density function $\Psi(y,t)$

$$\Psi(y,t) = \mathcal{N}\left(\mu_y(t), \sigma_y^2(t)\right) \tag{15}$$

where

$$\mu_y(t) = \int_{-\infty}^{+\infty} y\psi(y,t)dy$$

$$\sigma_y^2(t) = \int_{-\infty}^{+\infty} \left(y-\mu_y(t)\right)^2\psi(y,t)dy \tag{16}$$

Table 1. Acronyms of Different Models and Parameter Estimation Methods Used

GZ-ML	Gompertz model with parameters estimated through Maximum Likelihood Estimation
LG-LS	Logistic model with parameters estimated through Least Square Method
LG-ML	Logistic model with parameters estimated through Maximum Likelihood Estimation

The first moment follows the deterministic Gompertz equation (in logarithmic scale), and, therefore, the analytical solution is given by the following equation

$$\mu_y(t) = K\left[1-\left(1-\frac{\mu_0}{K}\right)e^{-\frac{r}{K}(t-t_0)}\right] \tag{17}$$

where K is the average asymptotic size of the crystals dimension, r is the growth rate, t_0 is the starting time of the run and μ_0 is the initial mean size of crystals at $t = t_0$.

The second moment can be described by considering the analogy between the FPE and the Kalman filter[17] for a linear process, and then the Riccati's equation will describe the variance changes in time. Writing the Riccati's equation for a Kalman filter for one single state without measurement, we have

$$\frac{d\sigma_y^2(t)}{dt} = q^2 + 2A\sigma_y^2(t) \tag{18}$$

where $\sigma_y^2(t)$ is the variance, $q2 = 2D$ is the noise intensity, and $A = -\frac{r}{K}$ is the coefficient of the state variable of the system. Thus, the analytical solution of the variance $\sigma^2(t)$ with respect to the time, is given by

$$\sigma_y^2(t) = \sigma_0^2 e^{-2\frac{r}{K}(t-t_0)} + \frac{DK}{r}\left[1-e^{-2\frac{r}{K}(t-t_0)}\right] \tag{19}$$

Thus, the analytical solution of the Eq. 13 is eventually

$$\Psi(y,t) = \frac{1}{\sigma_y(t)\sqrt{2\pi}} exp\left[-\frac{\left(y-\mu_y(t)\right)^2}{2\sigma_y^2(t)}\right] \tag{20}$$

where the time evolution of $\mu_y(t)$ and $\sigma_y(t)^2$ are given in Eqs. 17 and 19, respectively. A different demonstration of the analytical solution (Eq. 20) can be found elsewhere.[21]

Furthermore, it can be noticed that the analytical solution is a log-normal distribution when rewritten in the linear scale L

$$\Psi(L,t) = \frac{1}{\sigma_y(t)\sqrt{2\pi}L} exp\left[-\frac{\left(log(L)-\mu_y(t)\right)^2}{2\sigma_y^2(t)}\right] \quad L \geq 0 \tag{21}$$

Table 2. Inferred Model Parameters

	LG-LS			LG-ML			GZ-ML			
	LFR	**MFR**	**HFR**	**LFR**	**MFR**	**HFR**		**LFR**	**MFR**	**HFR**
r	1.254	1.354	1.902	1.474	1.755	1.922	**v**	4.720	5.180	8.659
K	4.840	4.683	4.635	4.786	4.635	4.607	**K**	4.795	4.631	4.585
D	0.112	0.138	0.178	0.125	0.176	0.147	**D**	0.088	0.106	0.156

The first two moments of the distribution $\Psi(L,t)$ in the linear scale can then be evaluated as

$$\mu_L(t) = \int_0^\infty L\Psi(L,t)dL = e^{\mu_y(t)+\frac{\sigma_y(t)^2}{2}} \tag{22}$$

$$\sigma_L^2(t) = \int_0^\infty (L-\mu_L(t))^2\Psi(L,t)dL = e^{2\mu_y(t)+\sigma_y^2(t)}\left(e^{\sigma_y^2(t)}-1\right) \tag{23}$$

Equations 17, 19 and 20 (or conversely 21, 22 and 23) provide a time evolution of the PSD as function of the model parameters in terms of the first two stochastic moments (mean size of crystals and variance of the PSD) available in an analytical form, which can be a valuable information for the design of proper offline and/or online model based control strategies.

Experiments

A set of experiments was carried out for parameter estimation as well as for model validations for the NaCl-water-ethanol antisolvent crystallization system. The experiments were carried in a bench-scale crystallizer that was kept at a fixed temperature. Only purified water, reagent grade sodium chloride (99.5%) and 190 proof ethanol were used. The experimental setup and procedure are described as follows.

Experimental setup

The experimental rig is made up of liter glass, cylindrical crystallizer submerged in a temperature controlled bath.[19] The temperature in the bath is measured using an RTD probe, which is wired up to a slave temperature control system capable of heating and cooling. In similar fashion, the antisolvent addition is carried out by a slave peristaltic pump. The master control is performed by a computer control system that is wired up to the slave temperature and flow rate controllers, respectively. The desired set points are set by the master controller. All relevant process variables are recorded. Crystal-size samples are evaluated by visual inspection of images taken using a digital camera mounted in a stereomicroscope at 25x magnification. The data acquisition procedure is schematically represented in Figure 1: the images are processed by means of sizing computer software (Amscope®), the crystals captured by the image are taken one by one through visual inspection and their size is evaluated through manual detection of the crystals edges. Typically, for each time, the analyzed crystal sample has dimensions between 150 and 300 elements.

Experimental procedure

At the startup condition, the crystallizer is loaded with an aqueous solution of NaCl made up of 34 g of NaCl in 100 g of water. The temperature is kept at 20°C. Then ethanol was added to the aqueous NaCl solution using a calibrated peristaltic pump. Three different antisolvent flow rates were implemented: $u_0 = 0.7$ mL/min (hereafter, referred as low feed rate: LFR), $u_0 = 1.5$ mL/min (medium feed rate: MFR) and $u_0 = 3.0$ mL/min (high-feed rate: HFR). Along the operation, 5 mL samples were taken in an infrequent fashion. Such samples are vacuum-filtered over filter paper and then dried in an oven at 50°C for the visual inspection.

Parameter Estimation

Following the procedure outlined by Grosso et al.[14,19] the calibration of the proposed models is carried out separately for every run. The set of parameters $\theta = [\log_{10}(D), r, K]$ is inferred using two different procedures, i.e., least-squares method (LS) on the kernel-based density function estimation and maximum likelihood estimation method (ML). It should be noted that $\log_{10}(D)$ is used instead of D in order to reduce the statistic correlation between the parameters.[16,19]

In the least-squares (LS) approach, the parameters in the model are estimated searching the minimum of the objective function $\Phi_{LS}(\theta)$ given by the distance between the theoretical PSD $\Psi(y,t;\theta)$ carried out from numerical integration of the model, Eq. 9, where $\theta = [\log_{10}(D), r, K]$, and the experimental PSD $\Psi^*(y)$ estimated through kernel-density based estimation[22]

$$\Psi^*(y) = \frac{1}{N\lambda}\sum_{i=0}^{N}\frac{1}{\sqrt{2\pi}}exp\left[-\frac{(y-m_i)^2}{2\lambda^2}\right] \tag{24}$$

In Eq. 17 m_i is the ith crystal-size value (in logarithmic scale) experimentally observed through visual inspection of the images, N is the crystals sample data dimension and λ is the bandwidth parameter, to be optimized for a satisfactory description of the distribution.[22] The distance between the distributions is evaluated at n different spatial location, and m different time values for every operating condition

Table 3. AIC (Akaike's Information Criterion) for LG-ML and GZ-ML Models

	LFR	**MFR**	**HFR**
LG-ML	620.28	959.20	266.64
GZ-ML	674.27	1081.08	298.86

Table 4. Skewness of the PSD in Logarithmic Scale at the End of Run for the Three Operability Conditions

	Experimental	**LG-LS**	**GZ-LS**
LFR	-0.2999	-0.128	0
MFR	-0.2002	-0.147	0
HFR	-0.4029	-0.139	0

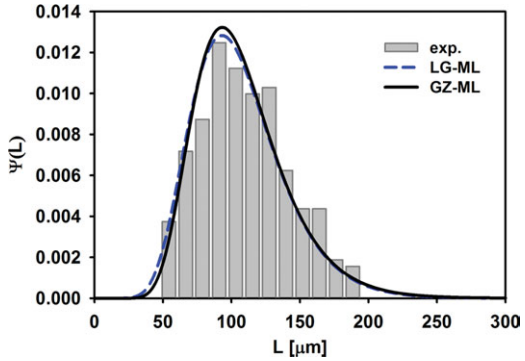

Figure 2. PSD comparison, in linear scale, for the MFR at the end of the experimental run: LG-ML model (dashed blue line); GZ-ML model (solid black line), and experimental PSD (vertical bars).

[Color figure can be viewed in the online issue, which is available at wileyonlinelibrary.com.]

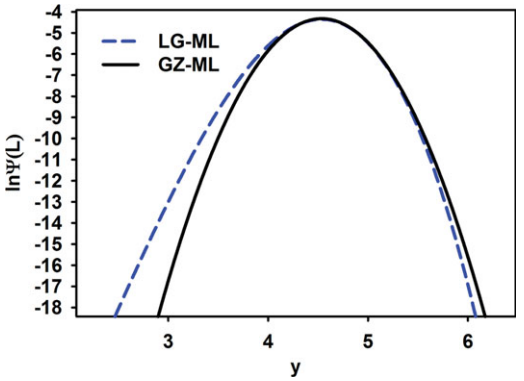

Figure 3. PSD comparison, in log–log scale: LG-ML (dashed blue line); GZ-ML (solid black line).

[Color figure can be viewed in the online issue, which is available at wileyonlinelibrary.com.]

$$\Phi_{LS}(\theta) = \sum_{i=1}^{m} \sum_{j=1}^{n} \left[\Psi(y_i, t_j; \theta) - \Psi^*(y_j, t_i) \right] \qquad (25)$$

More details on the procedure can be found elsewhere.[14,19]

Conversely, the maximum likelihood (ML) estimation approach, aims to determine the θ values that maximize the probability (likelihood) of the sample data measurements m_i. Thus, the parameters are inferred by searching the maximum of the log-likelihood function, that is the objective function $\Phi_{ML}(\theta)$ reported in Eq. 26

$$\Phi_{ML}(\theta) = logL(m_i, t_j; \theta) = \sum_{j=1}^{m} \sum_{i=1}^{n_j} log\left(\Psi(m_i, t_j; \theta)\right) \qquad (26)$$

ML estimation through Eq. 26 is rigorous if the crystal observations are assumed to be independent, which seems a reasonable hypothesis: the measurements technique here performed ensures that the outcome of the single observation will not influence the other ones. The ML has been already used to infer the parameters related to the process steady state[18] and it is demonstrated to give more efficient parameter estimation, that is, a minor number of experimental data are required to carry out an effective evaluation of the parameters, at least compared with the LS method. Indeed, since it achieves the Cramér-Rao lower bound, no asymptotically unbiased estimator has lower asymptotic mean squared error than the ML.[23] In addition, the introduction of possible errors in the evaluation of the experimental distribution (based on Eq. 24) is in this way circumvented. Thus, the onerous step in the experimental activity represented by the data acquisition through visual inspection can be eventually reduced.

In order to address a methodical analysis, the LG model will be calibrated and compared via both LS and ML algorithms. A Levenberg-Marquardt algorithm has been implemented to calculate the extremes of the objective functions $\Phi_{ML}(\theta)$ and $\Phi_{LS}(\theta)$. Table 1 summarizes the acronyms, hereafter, used to refer to the model and the model calibration procedure.

It should be remarked that the integration of the FPE-LG, with initial Gaussian distribution, would describe the evolution of a distribution that will be not more Gaussian as the time is evolving, being the drift term non linear [16], and possibly affecting the diffusion estimate of the parameter D. The selection of this initial condition is motivated by the fact that, due to the experimental method adopted, we could

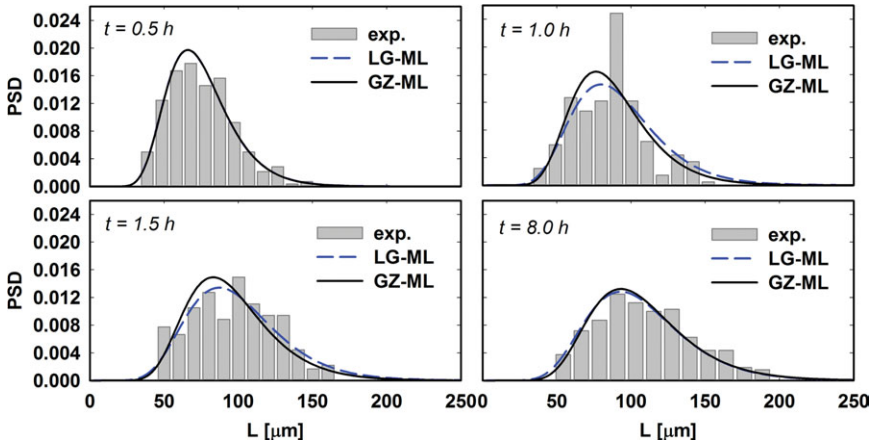

Figure 4. Transitory PSD comparison, in linear scale, for the MFR at different times (0.5 h, 1.0 h, 1.5 h, 8.0 h): LG-ML (dashed blue line); GZ-ML (solid black line) and represent the experimental PSD (vertical bars).

[Color figure can be viewed in the online issue, which is available at wileyonlinelibrary.com.]

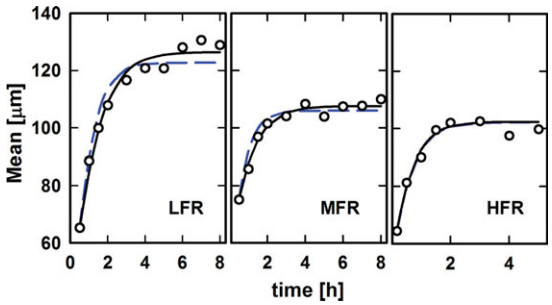

Figure 5. Linear mean size for LFR (a), MFR (b) and HFR (c): LG-ML (dashed blue line); GZ-ML (solid black line) and experimental values (white dots).

[Color figure can be viewed in the online issue, which is available at wileyonlinelibrary.com.]

have only a guess of the initial PSD, but a rather good mean crystal-size measurement. The latter is indeed more important in the parameters estimation issue since have a great influence on the growth rate constant. In any case, this approximation is not crucial since the characteristic time of the diffusion is faster than the one of the drift term, as could be seen by inspecting the characteristic times of the linear Eqs. 17 and 19, and considering that the drift term in the LG model is slightly nonlinear.

Table 2 reports the results obtained for LG-LS, already reported in the literature,[19] together with the LG-ML and the GZ-ML, for the different antisolvent flow rate values. It should be noted that the data estimation, using both methodologies, leads to slight differences among parameter values. In particular, small difference could be observed for the

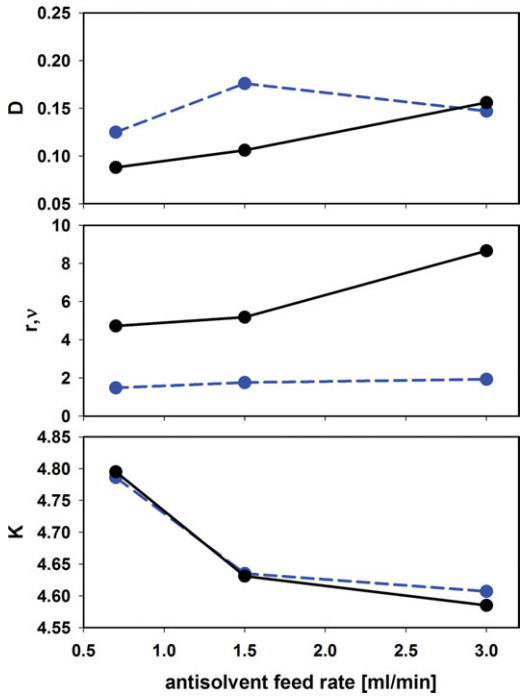

Figure 6. Parameter estimated for the two models: the dashed blue line is the LG-ML, and the solid black line is the GZ-ML.

[Color figure can be viewed in the online issue, which is available at wileyonlinelibrary.com.]

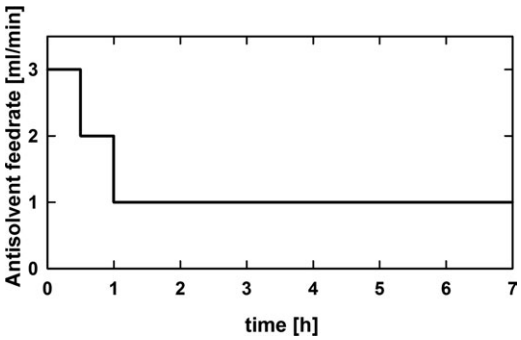

Figure 7. Experimental antisolvent addition policy used for the validation.

growth rate parameter r and for the pseudo-diffusivity coefficient D. The slight discrepancies can be also due to the introduction of the kernel basis function approximation in the LG-LS. On the other hand, the K parameter, representing the asymptotic value of the mean size of crystals in logarithmic scale, appears more robust to the approximation. The parameters show small difference between the GZ-ML and the LG-ML, except for the growth rate parameters r and v. This disagreement can be explained by observing that the growth rate for the GZ model is related defined as $v = rln(L_0) = rln(K)$.

Table 3 reports the Akaike information criterion (AIC) for both models studied, which gives a measure of the relative goodness of fit of a statistical model.[24] It was found that the values for the GZ model are slightly larger than the ones observed with the LG model, but they are, however, comparable. This aspect suggests some comments. Indeed, the better performance of the LG model (at least with respect to the GZ one) is a result somehow expected, since the linear model allows the description of only symmetric distributions $\Psi(y,t)$, whereas experimental observations suggest that some negative skewness in the y-data sample is always present and this outcome can be adequately captured only by nonlinear models. Nevertheless, the similar AIC values confirm that the linear model, for the case at hand, gives results close to the ones observed with the LG model, and it allows concluding that the GZ model provides a good description of the process. This result is encouraging for the development and the application of the GZ-ML model in the case of the optimization and the control of the crystallization system.

Figure 2 shows the obtained PSD, at the final time (end of the run), and at the medium flow rate (MFR) condition, for both LG-ML and GZ-ML. It is possible noticing that both models rather well describe the experimental distribution, but with small difference mainly observed in edges of the distributions. To better represent this aspect, the same distributions are represented in a log–log scale in Figure 3, where it is possible to appreciate the differences between the two distributions.

A further comparison between the two models can be accomplished by evaluating the distribution skewness, given by

$$\gamma(t) = \frac{\int_{-\infty}^{+\infty} (y - \mu_y(t))^3 \Psi(y,t) dy}{\left[\int_{-\infty}^{+\infty} (y - \mu_y(t))^2 \Psi(y,t) dy\right]^{3/2}} \tag{27}$$

for the fitted PSD, at the final time for all the operating conditions, whose values are reported in Table 4. The skewness values for the GZ-ML are obviously equal to zero,

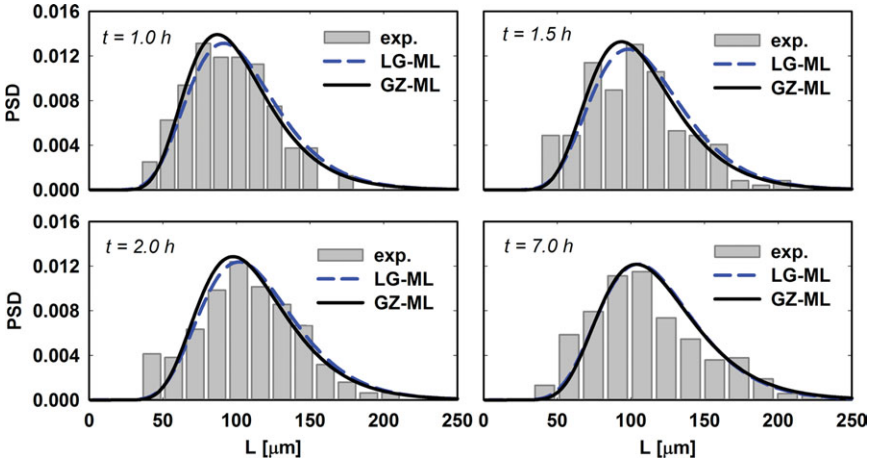

Figure 8. Transitory PSD comparison, in linear scale, for the MFR at different times (1.0 h, 1.5 h, 2.0 h, 7.0 h): LG-ML (dashed blue line); GZ-ML (solid black line) and represent the experimental PSD (vertical bars).

[Color figure can be viewed in the online issue, which is available at wileyonlinelibrary.com.]

since FPE with linear drift term preserves the Gaussianity introduced with the initial PSD.

A further test to appreciate the effectiveness of the GZ-ML approach is the comparison between the fitted PSD, by LG and GZ models (for both models the parameters were estimated through ML and they are given in Table 2, and the experimental histogram at four different sampling times for the MFR case, shown in Figure 4. The agreement between the experimental and the fitted PSDs are rather good with both models, the little difference is due by a zero value of the skewness parameter, that suggests the occurrence of some asymmetry in the PSD, but in the case studied this difference is imperceptible. Figure 5 shows the mean size of crystals evaluated with the LG and GZ models together with the experimental observations. The capability of the two models in describing the mean size of crystals in time, for the each operating condition, is rather excellent, confirming that the proposed model is a valid alternative to the nonlinear model.

Global Model Formulation and Validation

The proposed Fokker-Planck-based models do not have an explicit dependency of the control input u (i.e., antisolvent flow rate), although this variable does affect the process parameters. In order to use the model over the whole operational range a relationship between the parameters θ of the model, and the antisolvent flow rate has been developed following the same approach in Grosso et al.[14,19]

Consider our model, represented in Eq. 20, corresponding to a particular regime l (as defined by the antisolvent flow rate condition). Then, the local model at l can be expressed as

$$\Psi(y,t) = \frac{1}{\sigma_y(t)_l\sqrt{2\pi}} exp\left[-\frac{\left(y-\mu_y(t)_l\right)^2}{2\sigma_y^2(t)_l}\right] l = 1,2,3 \quad (28)$$

with

$$\mu_y(t)_l = K_l\left[1-\left(1-\frac{\mu_{y0}}{K_l}\right)e^{-\frac{v_l}{K_l}(t-t_0)}\right] \quad (29)$$

$$\sigma_y^2(t)_l = \sigma_{y0}^2 e^{-2\frac{v_l}{K_l}(t-t_0)} + \frac{D_l K_l}{v_l}\left[1-e^{-2\frac{v_l}{K_l}(t-t_0)}\right] \quad (30)$$

This local model structure parameterized by the vector θ is only valid within a particular operating regime and may not be valid in any other operating regime of the system. The local parameters θ are obtained through model identification as described above. Analyzing the dependency of the parameters with the antisolvent flow rate, Figure 6, the functionality of the model with the antisolvent flow rate is achieved by a piece-wise linear interpolation of the parameters for the different antisolvent flow rates. This functionality with the antisolvent flow rate allows the merger of multiple sets of parameters for different operating regimes to a single model across the operating envelope.

The model has been also validated by exploiting an experimental run that was not used for the calibration step. An antisolvent addition strategy, depicted in Figure 7, is used to validate the performance of the global model. The antisolvent addition policy starts at a high value of the flow (3 mL/min), in order to maximize nucleation, and it is reduced after 1 h with a few step changes to the final value $u_0 = 1$ mL/min, that was different from any flow rate used for calibration. Figure 8 illustrates the comparison between the predicted distributions, obtained using both models (LG and GZ) and the experimental density frequency at different time steps. The parameters, for both models, as function of the flow rate according to the piecewise interpolation are reported in Figure 6. From Figure 8 we can clearly notice that the agreement between the experimental and predicted time evolution of the PSD remains rather good even for the GZ model, thus, indicating that the proposed approach is a valid alternative to PBE models.

Conclusions

An alternative stochastic model for the description of antisolvent mediated crystal growth processes is introduced here. The size of each crystal is supposed to be subjected to a geometric Brownian motion, and its evolution in time is independent from the other crystals in the sample. A deterministic growth term is added to the stochastic model and is expressed as a Gompertz model. With this approach, the crystal size is a random variable, whose probability density evolution in time can be described in terms of a Fokker-Planck equation that, in this case, is amenable of analytical solution. In this regard, simple analytical relationships were

proposed to predict the crystal size distribution for the first time. Since the model parameters are function of the operating conditions and their solution is practically instantaneous these equations can be used for online control implementation.

Moreover, the maximum likelihood estimation method for the model parameters inference is introduced allowing obtaining the parameters directly from the observed data without resorting to a preliminary estimation of the experimental PSD through, e.g., the development of a kernel based function. In this way, the estimation error due by the introduction of the kernel basis function approximation is circumvented.

Validations against experimental data for the NaCl-water-ethanol antisolvent crystallization system were presented for a number of antisolvent flow rate conditions. The analytical solution of the model represents an encouraging way to implement a control system based on the process model. The slight differences obtained in term of skewness and AIC analysis are negligible for a control point of view and the direct utilization of the experimental data instead making a fitting of the experimental PSDs as shown a reasonable approach for the parameter estimation, without the introduction of further errors in the system.

Acknowledgments

J. Romagnoli kindly acknowledges Regione Sardegna for the support, through the program "Visiting Professor 2010" and the financial support by NSF Award #1132324.

Notation

A = coefficient of the Riccati equation, h^{-1}
D = diffusivity or pseudo-diffusivity constant for the FPE, h^{-1}
h = deterministic model used for the drift term of the FPE in linear scale
h' = deterministic model used for the drift term of the FPE in logarithmic scale
K = asymptotic dimension of crystals in logarithmic scale, for the rearranged Gompertz model and for the logistic model
l = subscript used to indicate the local model
L = characteristic dimension of crystals, μm
L_0 = characteristic dimension of crystals, evaluated at $t = t_0$, μm
m_i = mean-size measurement for the i-th crystal, in logarithmic scale
N = crystal sample dimension
$\mathcal{N}$ = normal or Gaussian distribution operator
q^2 = noise intensity of the Langevin equation
r = growth rate parameter for the Logistic and Gompertz model, h^{-1}
t = time variable, h
t' = perturbative time, h
t_0 = initial time for the integration of the FPE, corresponding to the first experimental sample taken, h
u_0 = antisolvente feed rate, mL/min
y = characteristic dimension of crystals in logarithmic scale, lnL

Greek letters

$\gamma(t)$ = skewness function
Γ = noise intensity for the model used to apply the Kalman filter derivation
δ = delta of Dirac
η = white noise
θ = vector of parameters
θ^* = vector of parameters to estimate using both methodologies
λ = bandwidth of the Kernel basis function
μ_{y0} = mean size of crystals in logarithmic scale, evaluated at $t = t_0$
$\mu_L(t)$ = time evolution function of the mean size of crystals in linear scale, μm
$\mu_y(t)$ = time evolution function of the mean size of crystals in logarithmic scale
v = growth rate parameter for the rearranged Gompertz model, h^{-1}
σ_{y0} = standard deviation of crystals in logarithmic scale, evaluated at $t = t_0$
σ^2_{y0} = variance of crystals in logarithmic scale, evaluated at $t = t_0$
$\sigma_y(t)$ = time evolution function of the standard deviation of crystals in logarithmic scale
$\sigma^2_L(t)$ = time evolution function of the variance of crystals in linear scale, μm^2
$\sigma^2_y(t)$ = time evolution function of the variance of crystals in logarithmic scale
Σ = noise intensity for the predicted equation used to apply the Kalman filter derivation
$\Psi(L,t)$ = dependent variable of the FPE in linear scale
$\Psi(y,t)$ = dependent variable of the FPE
$\Psi(y,t_0)$ = dependent variable of the FPE evaluated at $t = t_0$
$\Psi^*(y,t)$ = dependent variable of the experimental distribution

Literature Cited

1. Zhou GZ, Fujiwara M, Woo XY, Rusli E, Tung HH, Starbuck C, Davidson O, Ge Z, Braatz RD. Direct design of pharmaceutical antisolvent crystallization through concentration control. *Crystal Growth Des*. 2006;6:892–898.
2. Trifkovic M, Sheikhzadeh M, Rohani S. Kinetics estimation and single and multi-objective optimization of seeded, antisolvent, isothermal batch crystallize. *Ind Eng Chem Res*. 2008;47:1586–1595
3. Nowee SM, Abbas A, Romagnoli JA. Model-based optimal strategies for controlling particle size in anti-solvent crystallization operations. *Cryst Growth Des*. 2008;8:2698–2706.
4. Nowee SM, Abbas A, Romagnoli JA. Antisolvent crystallization: Model identification, experimental validation and dynamic simulation. *Chem Eng Sci*. 2008;63:5457–5467.
5. Nagy ZK, Fujiwara M, Braatz RD. Modelling and control of combined cooling and antisolvent crystallization processes, *J Proc Contr*. 2008;18:856–864.
6. Lindenberg C, Krattli M, Cornel J, Mazzotti M, Brozio J. Design and optimization of a combined cooling/antisolvent process. *Cryst Growth Des*. 2009;9:1124–1136.
7. Ramkrishna D. *Population Balances. Theory and Applications to Particulate Systems in Engineering*. San Diego, CA: Academic Press; 2000.
8. Panagiotis DC, Nael E-F, Mingheng L, Prashant M. Model-based control of particulate processes. *Chem Eng Sci*. 2008;63:1156–1172.
9. Woranee P, Paisan K, Amornchai A. Optimization and non-linear control of a batch crystallization process. *J Chin Inst Chem Eng*. 2008;39:249–256.
10. Woo XY, Nagy ZK, Tan RBH, Braatz RD. Adaptive concentration control of cooling and antisolvent crystallization with laser backscattering measurement. *Cryst Growth Des*. 2009;9(1):182–191.
11. Abu Bakar MRA, Nagy ZK, Saleemi AN, Rielly CD. The impact of direct nucleation control on crystal size distribution in pharmaceutical crystallization processes. *Cryst Growth Des*. 2009;9(3): 1378–1384.
12. Kee NCS, Tan RBH, Braatz RD. Selective mrystallization of the metastable α-form of L-glutamic acid using concentration feedback control. *Cryst Growth Des*. 2009;9(7):3044–3051.
13. Mesbah A, Landlust J, Huesman AEM, Kramer HJM. A model-based control framework for industrial batch crystallization processes. *Chem Eng Res Des*. 2010;88:1223–1233.
14. Grosso M, Galàn O, Baratti R, Romagnoli JA. A stochastic formulation for the description of the crystal size distribution in antisolvent crystallization processes. *AIChE J*. 2010;56(8):2077–2087.
15. Sahoo S, Sahoo A, Shearer SFC. Dynamics of gompertzian tumor growth under environmental fluctuations. *Physica A*. 2010;389(6): 1197–1207.
16. Risken H. *The Fokker-Planck Equation: Methods of Solutions and Applications*. Berlin: Springer-Verlag; 1996.
17. Jazwnsky AH. *Stochastic Process and Filtering Theory*. London, UK: Academic Press, Inc; 1970.
18. Tronci S, Grosso M, Baratti R, Romagnoli JA. A stochastic approach for the prediction of psd in crystallization processes: Analytical solution for the asymptotic behavior and parameter estimation. *Comput Chem Eng*. 2011;35:2318–2325.
19. Grosso M, Cogoni G, Baratti R, Romagnoli JA. Stochastic approach for the prediction of psd in crystallization processes: formulation

and comparative assessment of different stochastic models. *Ind Eng Chem Res*. 2011;50:2133–2143.
20. Kile DE, Eberl DD, Hoch AR, Reddy MM. An assessment of calcite crystal growth mechanism based on crystal size distributions. *Geochim Cosmochim Acta*. 200,64:2937–2950.
21. Cogoni G, Grosso M, Baratti R, Romagnoli JA. Dynamic Evolution of PSD Modelled Using an Ornstein-Uhlenbeck Process Approach. In:Proceedings of the 18th IFAC World Congress, Milano, Italy. 28/08–02/09/2011;18:2839–2844.
22. Silverman BW. *Density Estimation for Statistics and Data Analysis*. London, UK: Chapman & Hall; 1986.
23. Papoulis A. *Random Variables and Stochastic Processes*. New York: McGraw-Hill, Inc; 1991.
24. Akaike H. A new look at the statistical model identification. *IEEE Trans Auto Contr*. 1974;AC-19:716–723.

Manuscript received May 17, 2011, and revision received Oct. 17, 2011.